

# Stochastic Optimal Control and Network Co-Design for Networked Control Systems

Kun Ji and Won-jong Kim\*

**Abstract:** In this paper, we develop a co-design methodology of stochastic optimal controllers and network parameters that optimizes the overall quality of control (QoC) in networked control systems (NCSs). A new dynamic model for NCSs is provided. The relationship between the system stability and performance and the sampling frequency is investigated, and the analysis of co-design of control and network parameters is presented to determine the working range of the sampling frequency in an NCS. This optimal sampling frequency range is derived based on the system dynamics and the network characteristics such as data rate, time-delay upper bound, data-packet size, and device processing time. With the optimal sampling frequency, stochastic optimal controllers are designed to improve the overall QoC in an NCS. This co-design methodology is a useful rule of thumb to choose the network and control parameters for NCS implementation. The feasibility and effectiveness of this co-design methodology is verified experimentally by our NCS test bed, a ball magnetic-levitation (maglev) system.

**Keywords:** Co-design, networked control system, optimal control, quality of control.

## 1. INTRODUCTION

Ever-increasing computational capabilities and bandwidths in the networking technology enabled researchers to develop NCSs to implement distributed control schemes from a distance [1-6]. Unlike conventional control systems, an NCS essentially comprises multiple nodes communicating with each other over communication networks. The analysis and design of an NCS with randomly varying delays is complicated and still an open research field [1]. The use of network in a control system introduces bandwidth constraints and latencies, and interesting results were reported in the literature to handle this problem recently. Kweon *et al.* [2] proposed an adaptive traffic smoothing method to achieve real-time communication over the Ethernet. Network scheduling problems were studied by Hong [3] and Tovar *et al.* [4]. Walsh *et al.* [5] proposed a try-once-discard (TOD) protocol and analyzed the stability of

NCSs with limited communications. The stability regions of NCSs were proposed using a hybrid systems technique in [5,6]. There are some achievements in the design of NCSs with delay that is shorter than the sampling period [7-9] or longer than the sampling period [10,11]. Luis and Panos [8] proposed model-based control to handle network constraints. They only considered the case with the network between the sensor node and the controller node. A system design chart was proposed in [12] as a guideline for NCS design. For the stability analysis, the control law in use was designed in advance without considering the presence of the network in all of the above references. No controller synthesis method was given for NCSs.

Because the key for NCSs is that almost no local control action can be taken in isolation from the rest of the system and that the design parameters of feedback control and real-time communication systems are interdependent, the successful design and implementation of an NCS requires an appropriate integration of control systems, real-time systems, and network communication systems through co-design [13-15]. In [13], Branicky *et al.* introduced the idea of NCS co-simulation for co-design. They proposed techniques to simulate NCSs, and the simulation results could be used to refine the design of both the network and the control system. Control and network scheduling co-design was proposed in [14,15]. In this paper, we focus on estimating the optimal sampling frequency and optimal control with the consideration of the network-induced time delay.

---

Manuscript received November 23, 2006; revised May 1, 2007; accepted August 7, 2007. Recommended by Editorial Board member Huanshui Zhang under the direction of Editor Jin Young Choi. This material is based upon work supported by the National Science Foundation under Grant No. CMS-0116642.

Kun Ji is with Siemens Technology to Business Center, 1995 University Ave., Berkeley, CA 94704, U.S.A. (e-mail: kunjitam@gmail.com).

Won-jong Kim is with the Department of Mechanical Engineering, Texas A&M University, College Station, TX 77843-3123, U.S.A. (e-mail: wjkim@tamu.edu).

\* Corresponding author.

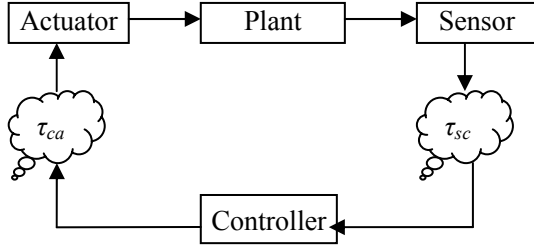


Fig. 1. An NCS with network-induced time delays.

We consider an NCS framework as shown in Fig. 1. The feedback control loop is closed over the network. Because of the limited network bandwidth, two classes of communication delays are included in this framework: (1) sensor-to-controller delay  $\tau_{sc}$  and (2) controller-to-actuator delay  $\tau_{ca}$ . We assume that the necessary time for analog-to-digital (AD) conversion at the sensor node and digital-to-analog (DA) conversion at the actuator node is included into the device processing time to be discussed in Section 3. Similarly an NCS configuration with a wireless computer network was proposed in [16].

This paper is organized as follows. The NCS model and the problem statement are presented in Section 2. The network and control co-design consideration is presented in Section 3. A sufficient condition for exponentially asymptotical stability is presented, and the upper bound of the time delay that can be accommodated and maximum and minimum sampling frequencies are also determined in this section. Approaches of stochastic optimal controller design for NCSs are proposed in Section 4. Experimental-verification results are given in Section 5.

## 2. PROBLEM STATEMENT

### 2.1. Modeling of NCSs

With the consideration of network-induced time delay and data-packet loss in data transmission, the NCS shown in Fig. 1 is described by the following dynamic model.

$$\begin{aligned} \dot{x}(t) &= Ax(t) + Bu(t) + v(t), \\ y(t) &= Cx(t) + w(t), \\ u(t) &= u(h_k), \quad t \in [h_k + \tau_k, h_{k+1} + \tau_{k+1}), \end{aligned} \quad (1)$$

where  $x(t) \in R^n$  is the state vector,  $u(t) \in R^m$  is the control input vector,  $y(t) \in R^q$  is the output vector, and  $A$ ,  $B$ , and  $C$  are known real constant matrices of appropriate dimensions. With the sensor sampling period  $h$ ,  $h_k$  denotes a certain sampling instant with  $h_k = i_k h$ ,  $k = 0, 1, 2, \dots$ , where  $k$  is the index of the sensor sampling instants, and  $i_k \in \{0, 1, 2, 3, \dots\}$  is the index of the arrived packets at the actuator node. The

difference between  $k$  and  $i_k$  is discussed in Remarks 1 and 3 below. The parameter  $\tau_k$  denotes the time delay from the instant  $h_k$  when the sensor samples data to the instant when the actuator actuates the control input  $u(h_k)$ . We have  $\tau_k = \tau_{sc} + \tau_{ca}$  for a fixed control law [6]. Let  $t_0$  denote the instant when the control system is

activated for the first time, then  $\bigcup_{k=1}^{\infty} [h_k + \tau_k, h_{k+1} + \tau_{k+1}) = [t_0, \infty)$ ,  $t_0 \geq 0$ . We define the following initial condition function

$$x(t) = \theta(t), \quad t \in [t_0 - \tau_0, t_0). \quad (2)$$

In this paper, we make the following assumptions:

1. The sensor is clock-driven while the controller and the actuator are event-driven.
2. The network-induced time delay is time varying with an unknown probability distribution function but bounded. Previous time delays up to  $h_{k-1}$  are known at  $h_k$ , which can be realized by placing a time stamp on every data packet to be sent through the network.
3. The plant noise  $v(t)$  and the sensor noise  $w(t)$  are zero-mean white Gaussian noises (WGNs) with  $E\{v^T(i)v(j)\} = R_1\delta(i, j)$ ,  $E\{w^T(i)w(j)\} = R_2\delta(i, j)$ , where  $R_1 \geq 0, R_2 \geq 0$ , and  $\delta(i, j) = 1$  when  $i = j$ ,  $\delta(i, j) = 0$  when  $i \neq j$ . These noises are independent of previous states, control inputs, and network-induced time delays.
4. There is no control input before the first control signal reaches the plant, i.e.,  $u(t) = 0$  for  $t < t_0$ .

**Remark 1:**  $i_k \in \{0, 1, 2, 3, \dots\}$ , i.e.,  $\{i_0, i_1, i_2, i_3, \dots\}$  is a subset of  $\{0, 1, 2, 3, \dots\}$ . From Assumption 2 we assume that the time delay is bounded, then there exist constants  $\tau > 0$  and  $H > 0$ , such that  $\tau_k < h_{k+1} + \tau_{k+1} - h_k \leq \tau = Hh, k = 1, 2, \dots$ . There are several special cases in model (1-2):

1. If  $i_{k+1} = i_k + 1$ , then  $\tau_k < h + \tau_{k+1}$ . It includes two further special cases: (1)  $\tau_k = \tau_0$  (the time delay is a constant); and (2)  $\tau_k < h$  (the time delay is less than one sampling period).
2. If  $i_k = k$ , i.e.,  $\{i_0, i_1, i_2, \dots, i_k\} = \{0, 1, 2, \dots, k\}$ , there is no data-packet loss in data transmission. Otherwise, missing integers indicate the lost data packets.
3. It is not required that  $i_k < i_{k+1}$ . If  $i_k > i_{k+1}$ , there is out-of-order data transmission between the  $i_k$ -th data packet and the  $i_{k+1}$ -th data packet.

Therefore, (1-2) are a general form of the NCS model where the effects of the network-induced time delay, data-packet loss, and out-of-order data transmission are all included.

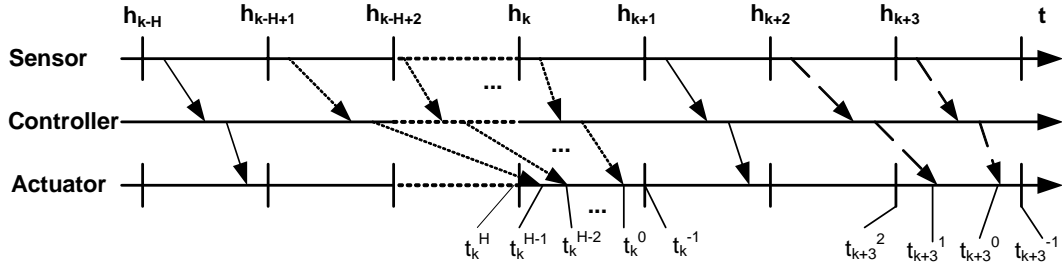


Fig. 2. Timing diagram of data packets transmission.

Two types of controllers are considered.

1. Full-state-feedback controller:

$$u(t) = Kx(h_k), \quad t \in [h_k + \tau_k, h_{k+1} + \tau_{k+1}). \quad (3)$$

2. Estimated-state-feedback controller:

$$\begin{aligned} \dot{\hat{x}}(t) &= A\hat{x}(t) + Bu(t) + L[y(t) - C\hat{x}(t)] \\ u(t) &= K\hat{x}(h_k), \quad t \in [h_k + \tau_k, h_{k+1} + \tau_{k+1}), \end{aligned} \quad (4)$$

where  $K \in R^{m \times n}$  is a constant matrix.

**Remark 2:** The control input  $u(t)$  to the plant is piecewise constant during a sampling interval  $[h_k, h_{k+1})$ . From Assumptions 1 and 2, and from Remark 1,  $\tau_k < Hh$ ,  $k=1,2,\dots$ . Thus there can be at most  $H$  control inputs in one sampling interval. A typical timing diagram of data packets transmitted in the control loop is illustrated in Fig. 2. The solid arrows denote the control input delayed less than one sampling period. The dotted arrows denote that there are  $H$  delayed control inputs actuated at the actuator node in the sampling interval  $[h_k, h_{k+1})$ . The dashed arrows denote that there are 2 control inputs actuated at the actuator node in the sampling interval  $[h_{k+3}, h_{k+4})$ . In the sampling interval  $[h_k, h_{k+1})$ , the control inputs arrive at the actuator node at the random instants  $h_k + t_k^j$ , where  $0 \leq t_k^j \leq h, j \leq H$ .

In order to analyze the closed-loop system in the discrete-time domain, we use the following state-space solution of a set of first-order matrix differential equations to discretize the continuous-time plant dynamic model (1) [17].

$$\begin{aligned} x(t) &= \exp(A(t-t_0))x(t_0) \\ &+ \int_{t_0}^t \exp(A(t-s))Bu(s)ds. \end{aligned} \quad (5)$$

Assuming no out-of-order data transmission and substituting (5) to (1) with  $t = h_{k+1}$  and  $t_0 = h_k$  yields

$$\begin{aligned} x(i_{k+1}) &= A_d(h)x(i_k) + \sum_{j=0}^l B_k^j(h)u(i_{k-i}) + v(i_k), \\ y(i_k) &= Cx(i_k) + w(i_k), \quad l=1,2,\dots,H, \end{aligned} \quad (6)$$

where

$$\begin{aligned} A_d(h) &= e^{Ah}, \\ B_k^j(h) &= \int_{t_k^j}^{t_k^{j-1}} \exp(A(h-s))dsB, \quad t_k^l = 0, \quad t_k^{-1} = h, \\ v(i_k) &= \int_{h_k}^{h_{k+1}} e^{A(h_{k+1}-s)}v(s)ds, \quad w(i_k) = w(h_k). \end{aligned}$$

$v(i_k)$  and  $w(i_k)$  are still zero-mean WGNs.

## 2.2. Control and network co-design problem

An important point to consider in the design of an NCS as shown in Fig. 1 is that the dynamic behavior of the distributed architecture largely depends on the characteristics and performance parameters of the underlying network, such as medium-access protocol, data-transmission rate, and available communication bandwidth. Thus, NCS design is a multidisciplinary field that includes the co-design of control systems and network communication systems. As proposed in [12], the system performance of an NCS is affected by network characteristics, such as data-transmission rate, time delays, and data-packet losses. Thus in an NCS design, there exists a system performance chart as shown in Fig. 3, which is a modification of Fig. 1 in [12]. As the sampling frequency gets higher, the traffic load becomes heavier in a bandwidth-limited network. Then the possibility of longer time delay or

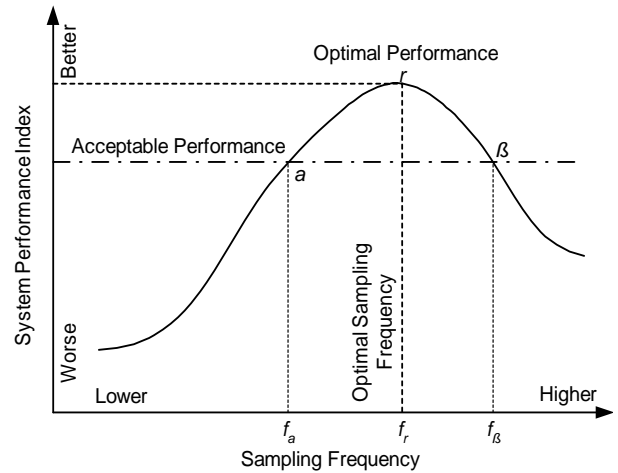


Fig. 3. System performance vs. sampling frequency, modified after [12].

more data-packet loss increases. Thus there exist the optimal performance point  $\gamma$  and the minimum acceptable performance points  $\alpha$  and  $\beta$  as denoted in Fig. 3. Based on the work in [12], we define the acceptable performance as stability, i.e., the interval  $(f_\alpha, f_\beta)$  in Fig. 3 is the working range of the sampling frequency with which the system can be stabilized.

### 2.3. Stochastic optimal control problem for NCSs

To improve the overall NCS performance, an optimal control problem is formulated in Section 4.

## 3. NETWORK AND CONTROL CO-DESIGN CONSIDERATION

### 3.1. Sufficient stability condition and lowest allowable sampling frequency $f_a$

First we present a controller design method for the system (1-2) with a full-state-feedback controller (3) and derive a sufficient stability condition based on a Lyapunov functional method. Then with the derived stability criteria, the maximum allowable value of the network-induced delay can be determined by solving a set of linear matrix inequalities (LMIs) [18]. Furthermore, the relationship among the lower bound on the data-transmission rate, the sampling frequency, and the network-induced delay can also be determined by using this sufficient condition. The frequency  $f_a$  can thus be determined by the above relationship.

**Lemma 1:** For any vectors  $u, v \in R^n$  and any real symmetric positive-definite matrix  $P \in R^{n \times n}$ , the following inequality holds.

$$-2u^T v \leq u^T P^{-1} u + v^T P v. \quad (7)$$

**Proof:** Introduce the matrix

$$N = P^{-\frac{1}{2}} u + P^{\frac{1}{2}} v.$$

Then,

$$\begin{aligned} N^T N &= (P^{-\frac{1}{2}} u + P^{\frac{1}{2}} v)^T (P^{-\frac{1}{2}} u + P^{\frac{1}{2}} v) \\ &= u^T P^{-1} u + v^T P v + 2u^T v \geq 0. \end{aligned}$$

**Theorem 1:** Given scalars  $\tau > 0$  and  $\lambda_i > 0$  ( $i = 2, 3, 4$ ), the closed-loop system (1-3) is exponentially asymptotically stable with a control input of  $K = YX^{-T}$  if there exist real symmetric positive-definite matrices  $P$  and  $Q$ , a nonsingular matrix  $X$ , and matrices  $Y$  and  $Z_j$  ( $j = 1, 2, 3, 4$ ) of appropriate dimensions such that the following LMI (8) holds.

$$\begin{bmatrix} M_{11}(X, Z_1) & M_{12}(X, Y, Z_1, Z_2, \lambda_2) & M_{13}(X, P, Z_3, \lambda_3) \\ * & M_{22}(Y, Z_2, \lambda_2) & M_{23}(X, Y, Z_3, \lambda_2, \lambda_3) \\ * & * & M_{33}(X, Q, \lambda_3, \tau) \\ * & * & * \\ * & * & * \end{bmatrix} < 0, \quad (8)$$

$$\begin{bmatrix} M_{14}(Z_4, X) & M_{15}(Z_1, \tau) \\ M_{24}(Z_4, X, \lambda_2) & M_{25}(Z_2, \tau) \\ M_{34}(X, \lambda_3, \lambda_4) & M_{35}(Z_3, \tau) \\ M_{44}(X, \lambda_4) & M_{45}(Z_4, \tau) \\ * & M_{55}(Q, \tau) \end{bmatrix} < 0, \quad (8)$$

where

$$M_{11}(X, Z_1) = Z_1 + Z_1^T - AX^T - XA^T, \quad (9)$$

$$M_{12}(X, Y, Z_1, Z_2, \lambda_2) = Z_2^T - Z_1 - \lambda_2 XA^T - BY, \quad (10)$$

$$M_{13}(X, P, Z_3, \lambda_3) = Z_3^T - \lambda_3 XA^T + X^T + P, \quad (11)$$

$$M_{14}(Z_4, X) = Z_4 - X^T - \lambda_4 XA^T, \quad (12)$$

$$M_{15}(Z_1, \tau) = \tau Z_1, \quad (13)$$

$$M_{22}(Y, Z_2, \lambda_2) = -Z_2 - Z_2^T - \lambda_2 (BY + Y^T B^T), \quad (14)$$

$$M_{23}(X, Y, Z_3, \lambda_2, \lambda_3) = -Z_3^T + \lambda_2 X^T - \lambda_3 Y^T B^T, \quad (15)$$

$$M_{24}(Z_4, X, \lambda_2) = -Z_4 - \lambda_2 X^T - \lambda_4 Y^T B^T, \quad (16)$$

$$M_{25}(Z_2, \tau) = \tau Z_2, \quad (17)$$

$$M_{33}(X, Q, \lambda_3, \tau) = \lambda_3 (X + X^T) + \tau Q, \quad (18)$$

$$M_{34}(X, \lambda_3, \lambda_4) = (\lambda_4 - \lambda_3) X^T, \quad (19)$$

$$M_{35}(Z_3, \tau) = \tau Z_3, \quad (20)$$

$$M_{44}(X, \lambda_4) = -2\lambda_4 X^T, \quad (21)$$

$$M_{45}(Z_4, \tau) = \tau Z_4, \quad (22)$$

$$M_{55}(Q, \tau) = -\tau Q. \quad (23)$$

**Proof:** Consider the following Lyapunov function

$$V(t) = x^T(t) \hat{P} x(t) + \int_{t-\tau}^t \int_v^t \dot{x}^T(s) \hat{Q} \dot{x}(s) ds dv, \quad (24)$$

where  $\hat{P}$  and  $\hat{Q}$  are real symmetric positive definite matrices. With the following formulae (25-28), where  $\lfloor \cdot \rfloor$  is the floor function,

$$\int_{h_k}^t \dot{x}(v) dv = x(t) - x(h_k), \quad (25)$$

$$\dot{x}(t) = \lim_{\delta \rightarrow 0^+} \sup \frac{x(t+\delta) - x(t)}{\delta}, \quad (26)$$

$$\begin{aligned} & \int_{t-\tau}^t \dot{x}^T(v) \hat{Q} \dot{x}(v) dv \\ &= \lim_{\delta \rightarrow 0^+} \delta \sum_{i=\lfloor \frac{t-\tau}{\delta} \rfloor}^k \left[ \dot{x}^T(i\delta) \hat{Q} \dot{x}(i\delta) \right], \quad t = k\delta, \end{aligned} \quad (27)$$

$$\begin{aligned} & \int_{t-\tau}^t \int_v^t \dot{x}^T(s) \hat{Q} \dot{x}(s) ds dv \\ &= \lim_{\delta \rightarrow 0^+} \delta^2 \sum_{j=\lfloor \frac{t-\tau}{\delta} \rfloor}^k \sum_{i=j}^k \left[ \dot{x}^T(i\delta) \hat{Q} \dot{x}(i\delta) \right]. \end{aligned} \quad (28)$$

and taking the time derivative of (24) for  $t \in [h_k + \tau_k, h_{k+1} + \tau_{k+1})$  yields

$$\begin{aligned}
 \dot{V}(t) &= 2x^T(t)\hat{P}\dot{x}(t) + \limsup_{\delta \rightarrow 0^+} \frac{\lim_{\delta \rightarrow 0^+} \left\{ \delta^2 \sum_{j=\lfloor k+1-\frac{\tau}{\delta} \rfloor}^{k+1} \sum_{i=j}^{k+1} [\dot{x}^T(i\delta)\hat{Q}\dot{x}(i\delta)] \right\} - \lim_{\delta \rightarrow 0^+} \left\{ \delta^2 \sum_{j=\lfloor k-\frac{\tau}{\delta} \rfloor}^k \sum_{i=j}^k [\dot{x}^T(i\delta)\hat{Q}\dot{x}(i\delta)] \right\}}{\delta} \\
 &= 2x^T(t)\hat{P}\dot{x}(t) + \lim_{\delta \rightarrow 0^+} \left\{ \delta \sum_{j=\lfloor k+1-\frac{\tau}{\delta} \rfloor}^{k+1} \sum_{i=j}^{k+1} [\dot{x}^T(i\delta)\hat{Q}\dot{x}(i\delta)] - \delta \sum_{j=\lfloor k-\frac{\tau}{\delta} \rfloor}^k \sum_{i=j}^k [\dot{x}^T(i\delta)\hat{Q}\dot{x}(i\delta)] \right\} \\
 &= 2x^T(t)\hat{P}\dot{x}(t) + \lim_{\delta \rightarrow 0^+} \left\{ \delta \frac{\tau}{\delta} \dot{x}^T[(k+1)\delta]\hat{Q}\dot{x}[(k+1)\delta] - \lim_{\delta \rightarrow 0^+} \left\{ \delta \sum_{i=\lfloor k-\frac{\tau}{\delta} \rfloor}^k [\dot{x}^T(i\delta)\hat{Q}\dot{x}(i\delta)] \right\} \right\}.
 \end{aligned}$$

Applying (27) to the above equation again, we obtain

$$\begin{aligned}
 \dot{V}(t) &= 2x^T(t)\hat{P}\dot{x}(t) + \tau \dot{x}^T(t)\hat{Q}\dot{x}(t) \\
 &\quad - \int_{t-\tau}^t \dot{x}^T(v)\hat{Q}\dot{x}(v)dv. \tag{29}
 \end{aligned}$$

From (1), (3), and (25), (29) can be rewritten as

$$\begin{aligned}
 \dot{V}(t) &= 2x^T(t)\hat{P}\dot{x}(t) + \tau \dot{x}^T(t)\hat{Q}\dot{x}(t) - \int_{t-\tau}^t \dot{x}^T(v)\hat{Q}\dot{x}(v)dv \\
 &\quad + 2 \left[ x^T(t)M_1 + x^T(h_k)M_2 + \dot{x}^T(t)M_3 + v^T(t)M_4 \right] \\
 &\quad \cdot \left[ x(t) - x(h_k) - \int_{h_k}^t \dot{x}(v)dv \right] \\
 &\quad + 2 \left[ x^T(t)N_1 + x^T(h_k)N_2 + \dot{x}^T(t)N_3 + v^T(t)N_4 \right] \\
 &\quad \cdot \left[ \dot{x}(t) - Ax(t) - BKx(h_k) - v(t) \right], \tag{30}
 \end{aligned}$$

where  $M_i$  and  $N_i$  ( $i = 1, 2, 3, 4$ ) are arbitrary symmetric matrices of appropriate dimensions.

From Remark 1 we assume  $\tau_k < h_{k+1} + \tau_{k+1} - h_k \leq \tau$ , then when  $t \in [h_k + \tau_k, h_{k+1} + \tau_{k+1})$ , we obtain  $t - \tau < h_k < t$ . Thus

$$-\int_{t-\tau}^t \dot{x}^T(v)\hat{Q}\dot{x}(v)dv \leq -\int_{h_k}^t \dot{x}^T(v)\hat{Q}\dot{x}(v)dv. \tag{31}$$

From Lemma 1, we obtain

$$\begin{aligned}
 &-2 \left[ x^T(t)M_1 + x^T(h_k)M_2 \right. \\
 &\quad \left. + \dot{x}^T(t)M_3 + v^T(t)M_4 \right] \int_{h_k}^t \dot{x}(v)dv \\
 &\leq \tau \tilde{x}^T(t)\tilde{M}\hat{Q}^{-1}\tilde{M}^T\tilde{x}(t) + \int_{h_k}^t \dot{x}^T(v)\hat{Q}\dot{x}(v)dv, \tag{32}
 \end{aligned}$$

where

$$\begin{aligned}
 \tilde{x}^T(t) &= \begin{bmatrix} x^T(t) & x^T(h_k) & \dot{x}^T(t) & v^T(t) \end{bmatrix}, \\
 \tilde{M} &= \begin{bmatrix} M_1 & M_2 & M_3 & M_4 \end{bmatrix}^T.
 \end{aligned}$$

Combining (30-32), we obtain

$$\dot{V}(t) \leq \tilde{x}^T(t) \Lambda \tilde{x}(t), \tag{33}$$

where  $\Lambda$  is shown below

Applying Schur complements, the condition  $\Lambda < 0$  is equivalent to the LMI (34) shown as follows.

$$\begin{aligned}
 \Lambda &= \begin{bmatrix} M_1 + M_1^T - N_1 A - A^T N_1^T & M_2^T - M_1 - A^T N_2^T - N_1 B K \\ * & -M_2 - M_2^T - N_2 B K - K^T B^T N_2^T \\ * & * \\ * & * \\ M_3^T - A^T N_3^T + N_1 + \hat{P} & M_4^T - N_1 - A^T N_4^T \\ -M_3^T + N_2 - K^T B^T N_3^T & -M_4^T - N_2 - K^T B^T N_4^T \\ N_3 + N_3^T + \tau \hat{Q} & N_4^T - N_3 \\ * & -N_4 - N_4^T \end{bmatrix} \\
 &\quad + \tau \tilde{M} \hat{Q}^{-1} \tilde{M}^T \\
 &= \begin{bmatrix} M_1 + M_1^T - N_1 A - A^T N_1^T & M_2^T - M_1 - A^T N_2^T - N_1 B K \\ * & -M_2 - M_2^T - N_2 B K - K^T B^T N_2^T \\ * & * \\ * & * \\ * & * \\ M_3^T - A^T N_3^T + N_1 + \hat{P} & M_4 - N_1 - A^T N_4^T & \tau M_1 \\ -M_3^T + N_2 - K^T B^T N_3^T & -M_4 - N_2 - K^T B^T N_4^T & \tau M_2 \\ N_3 + N_3^T + \tau \hat{Q} & N_4^T - N_3 & \tau M_3 \\ * & -N_4 - N_4^T & \tau M_4 \\ * & * & -\tau \hat{Q} \end{bmatrix} \\
 &\quad < 0 \tag{34}
 \end{aligned}$$

Define  $N = N_1, N_2 = \lambda_2 N, N_3 = \lambda_3 N, N_4 = \lambda_4 N, X = N^{-1}$ ,  $Y = KX^T, Z_i = XM_i X^T, P = X\hat{P}X^T$ , and let  $Q = X\hat{Q}X^T$ , then pre- and post-multiplying both sides of (34) with  $\text{diag}(X \ X \ X \ X \ X)$  and its transpose, respectively, we show that (34) is equivalent to (8).

**Remark 3:** From Remark 1, if  $h > h_{k+1}$ , there is out-of-order data transmission between the  $i_k$ -th data packet and the  $i_{k+1}$ -th data packet. That is, the new data packet containing  $x(h_k)$  may reach the plant before the old one containing  $x(h_{k+1})$ . Appropriately

discarding the outdated data packet can save network bandwidth and thus reduce the network-induced time delay, which in turn makes the system be able to tolerate a larger amount of data-packet loss. Therefore, it is necessary to time-stamp the data so that the sensor node can discard the outdated un-transmitted messages when the new packet is transmitted. The controller may also discard the outdated sensor data to reduce the network traffic between the controller node and the actuator node.

By Theorem 1, the upper bound of the time delay  $\tau$  that the system can accommodate can be determined by using a standard LMI solver. Furthermore, if we know the network characteristics and statistics, such as the lower bound of the data transmission rate and the device processing time, then the lowest allowable sampling frequency at Point  $\alpha$  in Fig. 3 can be estimated by

$$f_\alpha \approx 1/(\tau - T_d), \quad (35)$$

where  $T_d = T_t + T_p$  is the network-induced time delay that includes the data-transmission time  $T_t$  and the device processing time  $T_p$ .  $T_t$  can be estimated as  $T_t = L/R$  where  $R$  is the data rate in bytes per second for the current control application, and  $L$  is the average data-packet size in bytes. The device processing time  $T_p$  includes the time delays at the source and destination nodes. The processing time at the source node includes the preparing time  $T_{pre}$  (such as the time for AD or DA conversion) and the waiting time  $T_{wait}$ , and the processing time at the destination node (such as the time for AD or DA conversion) is the postprocessing time  $T_{post}$ . Thus the total device processing time  $T_p$  is given by [12]

$$T_p = T_{pre} + T_{wait} + T_{post}. \quad (36)$$

### 3.2. Maximum sampling frequency $f_\beta$

When the sampling frequency keeps increasing with a limited network bandwidth for the control application, the network traffic will be fully saturated and data-packet losses and longer time delays will occur frequently. If the longest time delay is longer than  $\tau$ , the system stability may be lost, in this case, we have  $(f_\beta \tau L)/R \approx \tau - T_p$ . Thus the highest allowable sampling frequency at Point  $\beta$  can be estimated by

$$f_\beta \approx (\tau - T_p)R/(\tau L). \quad (37)$$

### 3.3. Network bandwidth and optimal sampling frequency $f_\gamma$

The optimal sampling frequency can be estimated by further evaluating the system performance with different sampling frequencies selected from the range  $(f_\alpha, f_\beta)$ . An example of how to estimate this optimal sampling frequency is presented in Section 5.

The co-design procedure presented in this section is that we can find (1)  $\tau$  by Theorem 1, (2)  $h$  by the method to choose the sampling frequency presented in this section, and (3)  $H$  by the equation  $\tau = (H + 1)h$ . This  $H$  then can be used in the design of an optimal controller as presented in Section 4.

## 4. STOCHASTIC OPTIMAL CONTROLLER DESIGN FOR NCS

The improvement of NCS performance can be achieved in two ways [12]. One way is the minimization of device processing times and the improvement of network protocols to further guarantee the determinism of the data-transmission time as well as reduce the end-to-end delays. The designer should then pick a sampling frequency between points  $\alpha$  and  $\beta$  (best at  $\gamma$ ) in Fig. 3 and based on other necessary design constraints.

The other way for performance improvement is through advanced optimal controller design that can overcome the uncertainty in an NCS and achieve the best QoC. By Theorem 1 we can find  $\tau$ , and by the rule of thumb of choosing sampling frequency presented in Section 3, we can find the optimal sampling period  $h$ , then  $H$  can be found by the equation  $\tau = Hh$ . Based on the proposed model (6) and the value of  $H$ , a suboptimal controller design is developed to improve the overall NCS performance with the following two cases.

### 4.1. Full-state-feedback

In the system (6), let  $h^*$  be the optimal sampling period found in Section 3. We introduce a new augmented state variable as

$$z(i_k) = \begin{bmatrix} x^T(i_k) & u^T(i_{k-1}) & \dots & u^T(i_{k-H}) \end{bmatrix}^T \in R^{n+Hm},$$

then the augmented system can be expressed as follows

$$\begin{aligned} z(i_{k+1}) &= \Phi(i_k)z(i_k) + \Gamma(i_k)u(i_k) + \Sigma v(i_k), \\ y(i_k) &= C_0 x(i_k) + w(i_k), \end{aligned} \quad (38)$$

where

$$\begin{aligned} \Phi(i_k) &= \begin{bmatrix} A_d & B_{i_k}^1 & B_{i_k}^2 & \dots & B_{i_k}^{H-1} & B_{i_k}^H \\ 0 & 0 & 0 & \dots & 0 & 0 \\ 0 & I_m & 0 & \dots & 0 & 0 \\ \vdots & \vdots & \vdots & \ddots & \vdots & \vdots \\ 0 & 0 & 0 & \dots & I_m & 0 \end{bmatrix}, \\ \Gamma(i_k) &= \begin{bmatrix} B_{i_k}^0 \\ I_m \\ 0 \\ \vdots \\ 0 \end{bmatrix}, \quad \Sigma = \begin{bmatrix} I_m \\ 0 \\ 0 \\ \vdots \\ 0 \end{bmatrix}, \end{aligned} \quad (39)$$

$$C_0 = [C \ 0 \ \cdots \ 0],$$

$$A_d = A_d(h^*),$$

$$B_k^j = B_k^j(h^*),$$

where  $I_m$  is the  $m \times m$  identity matrix.

In this paper, we consider the problem of minimizing the following cost function

$$J(i_N) = E \left\{ z^T(i_N) Q_N z(i_N) + \sum_{k=0}^{N-1} [z^T(i_k) Q_0 z(i_k) + u^T(i_k) R_0 u(i_k)] \right\}, \quad (40)$$

where  $Q_N$  and  $Q_0$  are symmetric positive-semi-definite matrices, and  $R_0$  is a symmetric positive-definite matrix.

**Lemma 2:** Let  $E\{\cdot|y\}$  denote the conditional expectation given  $y$ . Assume that the function  $f(x, y, u) = E\{l(x, y, u)|y\}$  has a unique minimum with respect to  $u \in U$  for all  $x \in X$  and  $y \in Y$ . Let  $u^0(x, y)$  denote the value of  $u$  for which the minimum is achieved. Then we have

$$\begin{aligned} \min_{u(x,y)} E\{l(x, y, u)\} &= E\{l(x, y, u^0(x, y))\} \\ &= E\left\{ \min_{u(x,y)} E\{l(x, y, u)|y\} \right\}. \end{aligned}$$

**Proof:** Refer to [19].

**Theorem 2:** When the system has full state information, the control law that minimizes the cost function (40) is given by

$$u(i_k) = -L(i_k)[x^T(i_k) \ u^T(i_{k-1}) \ \cdots \ u^T(i_{k-H})]^T, \quad (41)$$

where  $L(i_k)$  is shown in (42),

$$\begin{aligned} L(i_k) &= \left[ R_0 + E\{ \Gamma^T(i_k) S(i_{k+1}) \Gamma(i_k) \} \right]^{-1} \\ &\quad E\{ \Gamma^T(i_k) S(i_{k+1}) \Phi(i_k) \}, \\ S(i_k) &= E\left\{ [\Phi(i_k) - \Gamma(i_k) L(i_k)]^T S(i_{k+1}) [\Phi(i_k) \right. \\ &\quad \left. - \Gamma(i_k) L(i_k)] \right\} + L^T(i_k) R_0 L(i_k) + Q_0, \\ S(i_N) &= Q_N. \end{aligned} \quad (42)$$

**Proof:** By repeatedly applying Lemma 2 to the cost function (40), we obtain the following Bellman equation:

$$J(i_k) = \min_u E\left\{ z^T(i_k) Q_0 z(i_k) + u^T(i_k) R_0 u(i_k) + J(i_{k+1})|z(i_k) \right\}. \quad (43)$$

We will prove that the solution to (43) is in the form

of (44).

$$J(i) = E\left\{ z^T(i) S(i) z(i) \right\} + \alpha(i), \quad (44)$$

where  $S(i)$  is a symmetric matrix and denotes the cost to go at time  $i$ , and  $\alpha(i)$  is the part of the cost function that is not affected by the control. The initial value at  $i = i_N$  is

$$\begin{aligned} J(i_N) &= \min_u E\left\{ z^T(i_N) Q_N z(i_N) | z(i_N) \right\} \\ &= E\left\{ z^T(i_N) Q_N z(i_N) \right\} \end{aligned}$$

with  $S(i_N) = Q_N$ . Thus (44) is the solution when  $i = i_N$ . If the solution holds when  $i = i_{k+1}$  and we can prove that it still holds when  $i = i_k$ , then we can prove that (44) is the solution to (43) by mathematical induction.

$$\begin{aligned} J(i_k) &= \min_{u(i_k)} E\left\{ z^T(i_k) Q_0 z(i_k) \right. \\ &\quad \left. + u^T(i_k) R_0 u(i_k) + J(i_{k+1})|z(i_k) \right\} \\ &= \min_{u(i_k)} E\left\{ z^T(i_k) Q_0 z(i_k) + u^T(i_k) R_0 u(i_k) \right. \\ &\quad \left. + E\{ [\Phi(i_k) z(i_k) + \Gamma(i_k) u(i_k)]^T S(i_{k+1}) \right. \\ &\quad \left. [\Phi(i_k) z(i_k) + \Gamma(i_k) u(i_k)] | z(i_k) \} \right. \\ &\quad \left. + \text{tr}[\Sigma^T S(i_{k+1}) \Sigma R_1] + \alpha(i_{k+1}) \right\}. \end{aligned} \quad (45)$$

Minimizing (45) with respect to  $u(i_k)$  gives the control law (41), and

$$\begin{aligned} J(i_k) &= E\left\{ z^T(i_k) \{ Q_0 + L(i_k)^T R_0 L(i_k) \right. \\ &\quad \left. + E\{ [\Phi(i_k) - \Gamma(i_k) L(i_k)]^T \right. \\ &\quad \left. S(i_{k+1}) [\Phi(i_k) - \Gamma(i_k) L(i_k)] \} \} z(i_k) \right\} \\ &\quad + \text{tr}(\Sigma^T S(i_{k+1}) \Sigma R_1) + \alpha(i_{k+1}) \\ &= E\left\{ z^T(i_k) S(i_k) z(i_k) \right\} + \alpha(i_k), \end{aligned}$$

where

$$\begin{aligned} S(i_k) &= E\left\{ [\Phi(i_k) - \Gamma(i_k) L(i_k)]^T S(i_{k+1}) [\Phi(i_k) \right. \\ &\quad \left. - \Gamma(i_k) L(i_k)] \right\} + L^T(i_k) R_0 L(i_k) + Q_0, \\ \alpha(i_k) &= \text{tr}[\Sigma^T S(i_{k+1}) \Sigma R_1] + \alpha(i_{k+1}), \\ L(i_k) &= \left[ R_0 + E\{ \Gamma^T(i_k) S(i_{k+1}) \Gamma(i_k) \} \right]^{-1} \\ &\quad E\{ \Gamma^T(i_k) S(i_{k+1}) \Phi(i_k) \}. \end{aligned}$$

Since  $Q_0$  and  $R_0$  are symmetric,  $S(i_k)$  is symmetric. Thus we can conclude that the solution to the Bellman equation (43) is (44) and complete the proof.

#### 4.2. Estimated-state-feedback control

When full state information is unavailable for the controller, a conventional way is to estimate unknown states with modified Kalman filters. A key issue with respect to this method is to verify whether the separation principle holds. Refer to [11] for a design idea of estimated-state feedback and output feedback. In [11], the optimal estimator of the system state is

presented when the system has partial state information and network-induced delay is longer than the sampling period. The separation principle is proved to still hold in such NCSs.

## 5. CASE STUDY

In this section, we provide an experimental verification of our co-design methodology with an NCS test bed containing a ball maglev system and illustrate the co-design of network and control system parameters.

### 5.1. System setup of the networked ball maglev test bed

The objective of the maglev test bed [20] is to levitate a steel ball at a predetermined steady-state equilibrium position with an electromagnet. The control input for the setup is the output current from a pulse-width-modulation (PWM) power amplifier, and the system output is the ball position measured by a CdS photocell. The transfer function from the PWM power amplifier input ( $V$ ) to the position sensor output ( $Y$ ) is described as [20]:

$$G(s) = \frac{Y(s)}{V(s)} = \frac{-0.02792}{0.0086s^2}. \quad (46)$$

The state-space model obtained by Matlab with minimum realization is given as

$$\begin{aligned} \dot{x}(t) &= \begin{bmatrix} 0 & 0 \\ 2 & 0 \end{bmatrix} x(t) + \begin{bmatrix} 1 \\ 0 \end{bmatrix} u(t) + v(t), \\ y(t) &= \begin{bmatrix} 0 & -1.6233 \end{bmatrix} x(t) + w(t). \end{aligned} \quad (47)$$

With this ball maglev test bed and the 100-Mbps Ethernet local area network (LAN) in our lab, we constructed an NCS shown in Fig. 4 with the system configuration as shown in Fig. 1. The plant PC with National Instruments PCI-6025E as the data acquisition card enables the ball maglev test bed to send out the sensor data and receive the control data through the LAN. The controller PC receives the sensor data, computes the control data, and then sends out the control data through the same LAN. Linux with real-time application interface (RTAI) runs on both PCs to ensure that the time-constrained events like sampling the sensor and actuating the electromagnet do not miss their deadlines [10].

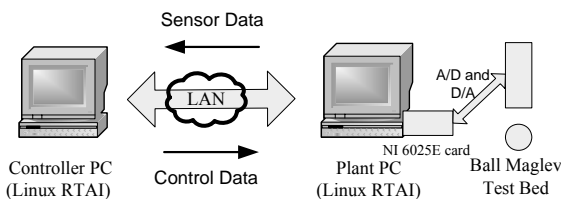


Fig. 4. An NCS with a ball maglev test bed.

### 5.2. Measurement of network characteristics

We collected the network traffic information of the Ethernet and the device processing time for data processing. A 76-byte-long data packet was sent from the plant PC to the controller PC and then came back from the controller PC to the plant PC. The mean value of the round-trip time delay was 0.23 ms, and we estimated that the data-transmission rate available for the test bed was about 2 Mbps. Based on the real-time operating system (Linux RTAI) implemented on both the controller PC and the plant PC [10], the device processing time for AD and DA conversions and control calculation could also be measured. For our NCS test bed, the device processing time  $T_p$  was estimated to be 0.8 ms based on the above measurement.

### 5.3. Control and network co-design

Applying Theorem 1 to the system model (47) and solving the LMI (8), we found that the upper bound of the time delay for (47) with a full-state feedback controller would be 0.051 s. By the discussion in Section 3, the working range of the sampling frequency can be estimated. From (35), we can estimate the minimum sampling frequency at Point  $\alpha$  for the ball maglev setup as  $f_{min} \approx 1/(\tau - T_t - T_p) = 1/(0.051 - 0.00023 - 0.0008) \approx 20$  Hz. Ethernet packets with minimum size (76 bytes) were used to carry the sensor data and the control data. Then from (37), we can estimate the maximum sampling frequency at point  $\beta$  as  $f_{max} \approx (\tau - T_p)R/(\tau L) = (0.051 - 0.0008) * 2 * 1048576 / (0.051 * 76 * 8) \approx 3.4$  kHz. Thus, based on the control and network co-design consideration, the allowable working range of the sampling frequency for this NCS test bed is from 20 Hz to 3.4 kHz. Since the ball maglev system has only one position sensor, full-state feedback is not available. Several output feedback controllers were designed to obtain the best control performance. A digital lead-lag controller designed in [20] to stabilize the ball maglev setup was given as

$$D(z) = 4.15 \times 10^4 \left( \frac{z^2 - 1.754z + 0.769}{z^2 - 0.782z - 0.13} \right). \quad (48)$$

Several experiments with the closed-loop ball maglev system (47-48) with various sampling frequencies were performed to verify the maximum constant time delay that the system can tolerate. A plot of the maximum constant time delays with respect to sampling frequencies is shown in Fig. 5. The best sampling frequency was found to be about 333.3 Hz, i.e. the best sampling period was 3 ms. It is worth mentioning that the shape of Fig. 5 does follow that of Fig. 3, and Fig. 5 is a performance chart specific to the ball maglev system.

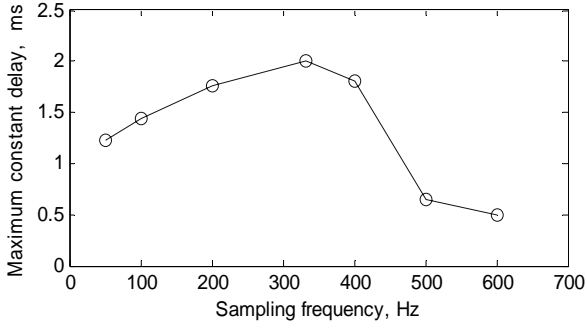


Fig. 5. Maximum allowable constant time delays with respect to sampling frequencies.

A discrete-time state-space model of the ball maglev system with the 3-ms sampling period is

$$\begin{aligned} x(i_{k+1}) &= \begin{bmatrix} 1 & 0 \\ 0.006 & 1 \end{bmatrix} x(i_k) + \begin{bmatrix} 0.003 \\ 0.000009 \end{bmatrix} u(i_k) \\ &\quad + v(i_k), \\ y(i_k) &= \begin{bmatrix} 0 & -1.6233 \end{bmatrix} x(i_k) + w(i_k). \end{aligned} \quad (49)$$

We found that the upper bound of network-induced time delay in our lab is less than two sampling periods, i.e.,  $H = 2$  in the system model (6). A practical output feedback controller for the system (49) was designed as

$$\begin{aligned} u(i_k) &= 0.78u(i_{k-1}) + 0.13u(i_{k-2}) - 18.92y(i_k) \\ &\quad + 33.19y(i_{k-1}) - 15.06y(i_{k-2}) + 0.24. \end{aligned} \quad (50)$$

This event-driven controller was implemented on our NCS test bed. All the sensor and control data are time stamped, any outdated data-packet is simply discarded based on the discussion in Remark 3 in Section 3.

#### 5.4. NCS quality of control

With the NCS test bed, several experiments were performed to check the QoC. The first experiment was the ball stabilization with the control loop closed over the Ethernet as shown in Fig. 4. The system response is shown in Fig. 6. From Fig. 6 we can see that the NCS test bed maintained its stability successfully, and that the ball

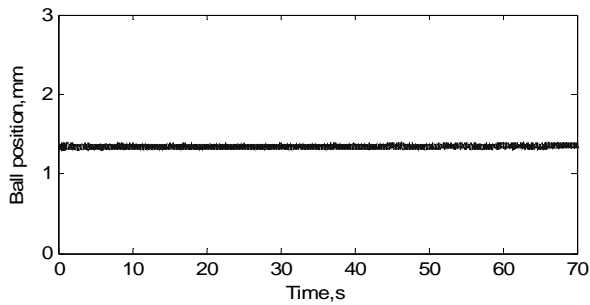
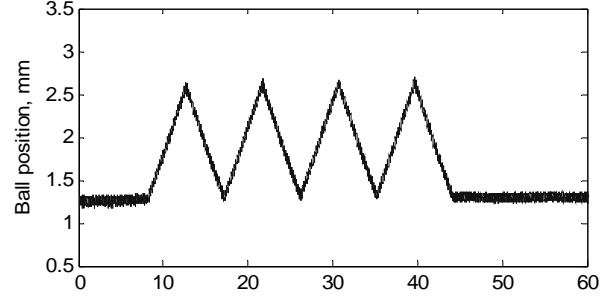
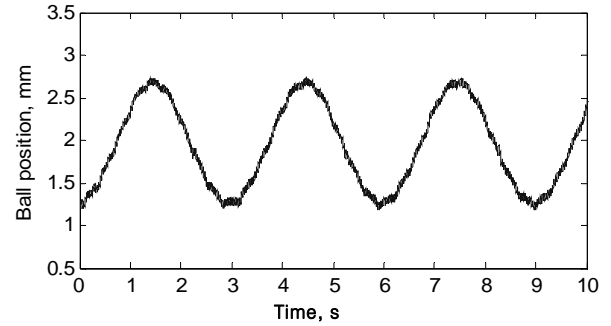


Fig. 6. Ball stabilization with the control loop closed over the Ethernet.



(a) Sawtooth



(b) Sinusoidal

Fig. 7. System responses to position commands.

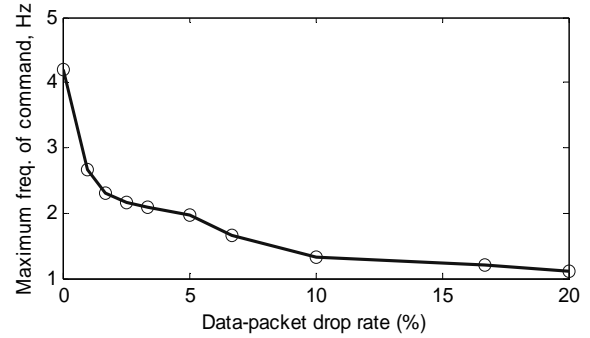


Fig. 8. Frequency of command that the ball can follow and packet loss rate.

was levitated at its equilibrium position.

The second set of experiments was to make the ball track commanded trajectories. Fig. 7(a) shows the system response to a saw-tooth position command, and Fig. 7(b), to a sinusoidal position command with a period of 3 s. The system maintained its stability and control performance even with the control loop closed over the Ethernet. Network-induced time delays and packet losses were successfully tolerated by the NCS test bed.

Then we introduced artificial data-packet losses for the purpose of confirming the robust stability and performance of our NCS. The maximum frequencies of the sinusoidal position commands that the ball can follow vs. various data-packet drop rates are plotted in Fig. 8. When the data-packet drop rate was greater than 10%, it was difficult for the NCS test bed to follow the command. In fact, the system would lose

its stability when the network-induced data-packet drop rate was greater than 20%.

## 6. CONCLUSIONS

The main contribution of this paper is to present a methodology for the analysis and design of an NCS that allows us to manage its QoC. We also addressed key co-design issues for NCSs including network parameters and control parameters, and networked control system performance was presented as a rule of thumb for NCS design.

We presented a new NCS model with the consideration of network-induced time delay, data-packet loss, and out-of-order data-packet transmission. Based on a design chart modified after [12], we also presented a quantitative method about how to determine the location of the performance degradation points in the NCS performance design chart. The optimal working range of the sampling frequency was also determined based on the locations of these points. To improve the overall QoC of NCSs, we described how optimal controllers can be designed for QoC optimization. The co-design procedure is that we can find (1)  $\tau$  by Theorem 1, (2)  $h$  by the method to choose the sampling frequency presented in Section 3, and (3)  $H$  by the equation  $\tau = Hh$ . This  $H$  then can be used in the design of an optimal controller as presented in Section 4.

We followed the co-design procedures developed in this paper and constructed an NCS test bed. With this NCS test bed, we experimentally verified the feasibility and effectiveness of our co-design methodology.

## REFERENCES

- [1] Y. Tipsuwan and M.-Y. Chow, "Control methodologies in networked control systems," *Control Engineering Practice*, vol. 11, no. 10, pp. 1099-1111, Feb. 2003.
- [2] S.-K. Kweon, K. G. Shin, and G. Workman, "Achieving real-time communication over Ethernet with adaptive traffic smoothing," *Proc. of IEEE Real-Time Tech. Appl. Symp.*, pp. 90-100, June 1999.
- [3] S. H. Hong, "Scheduling algorithm of data sampling times in the integrated communication and control systems," *IEEE Trans. Contr. Syst. Technol.*, vol. 3, no. 2, pp. 225-230, June 1995.
- [4] E. Tovar, F. Vasques, and A. Burns, "Supporting real-time distributed computer-controlled systems with multihop P-NET networks," *Control Engineering Practice*, vol. 7, no. 8, pp. 1015-1025, Aug. 1999.
- [5] G. C. Walsh, Y. Hong, and L. G. Bushnell, "Stability analysis of networked control system," *IEEE Trans. Contr. Syst. Technol.*, vol. 10, no. 3, pp. 438-446, May 2002.
- [6] W. Zhang, M. S. Branicky, and S. M. Phillips, "Stability of networked control systems," *IEEE Contr. Syst. Mag.*, vol. 21, no. 1, pp. 84-99, Feb. 2001.
- [7] J. Nilsson, *Real-Time Control Systems with Delays*, Ph.D. dissertation, Lund Inst. Technol., Lund, Sweden, 1998.
- [8] A. M. Luis and J. A. Panos, "Stability of model-based networked control systems with time-varying transmission times," *IEEE Trans. Automat. Contr.*, vol. 49, no. 9, pp. 1562-1572, Sep. 2004.
- [9] C. G. Graham, H. Hernan, E. Q. Daniel, and S. W. James, "A moving horizon approach to networked control system design," *IEEE Trans. Automat. Contr.*, vol. 49, no. 9, pp. 1427-1444, Sep. 2004.
- [10] K. Ji and W.-J. Kim, "Real-time control of networked control systems via Ethernet," *International Journal of Control, Automation, and Systems*, vol. 3, no. 4, pp. 591-600, Dec. 2005.
- [11] S. S. Hu and Q. X. Zhu, "Stochastic optimal control and analysis of stability of networked control systems with long delay," *Automatica*, vol. 39, no. 11, pp. 1877-1884, Nov. 2003.
- [12] F.-L. Lian, J. Moyne, and D. Tilbury, "Network design consideration for distributed control systems," *IEEE Trans. Contr. Syst. Technol.*, vol. 10, no. 2, pp. 297-307, Mar. 2002.
- [13] M. S. Branicky, V. Liberatore, and S. M. Phillips, "Networked control system co-simulation for co-design," *Proc. of American Control Conference*, pp. 3341-3346, June 2003.
- [14] L. Zhang and D. Hristu-Varsakelis, "Stabilization of networked control systems under feedback-based communication," *Proc. of American Control Conference*, pp. 2933-2938, June 2005.
- [15] K.-E. Årzén, A. Cervin, J. Eker, and L. Sha, "An introduction to control and scheduling co-design," *Proc. of the 39th IEEE Conference on Decision and Control*, pp. 4865-4870, Dec. 2000.
- [16] N. J. Ploplys, P. A. Kawka, and A. G. Alleyne, "Closed-loop control over wireless network," *IEEE Contr. Syst. Mag.*, vol. 24, no. 3, pp. 58-71, June 2004.
- [17] G. F. Franklin, J. D. Powell, and M. L. Workman, *Digital Control of Dynamic Systems*, 3rd ed., Addison-Wesley, Reading, MA, 1998.
- [18] S. Boyd, L. E. Ghaoui, E. Feron, and V. Balakrishnan, *Linear Matrix Inequalities in System and Control Theory*, SIAM, Philadelphia, PA, 1994.
- [19] K. J. Astrom, *Introduction to Stochastic Control Theory*, Academic Press, New York, 1970.

- [20] S. C. Paschall, II, *Design, Fabrication, and Control of a Single Actuator Magnetic Levitation System*, Senior Honors Thesis, Texas A&M University, College Station, TX, May 2002.



**Kun Ji** received the B.S. and M.S. degrees in Precision Instrumentation and Engineering from Tsinghua University, Beijing, China, in 1999 and 2002, respectively, and the Ph.D. degree in Mechanical Engineering from Texas A&M University, College Station, in 2006. He has been with Siemens Technology to Business

Center, Berkeley, where currently he is a Research Scientist. His research interests focus on analysis, design of networked control systems, real-time control systems, wireless sensor networks and precision mechatronics systems.



**Won-jong Kim** received the B.S. (*summa cum laude*) and M.S. degrees in Control and Instrumentation Engineering from Seoul National University, Seoul, Korea, in 1989 and 1991, respectively, and the Ph.D. degree in Electrical Engineering and Computer Science from Massachusetts Institute of Technology (MIT),

Cambridge, in 1997. Since 2000, he has been with the Department of Mechanical Engineering, Texas A&M University (TAMU), College Station, where currently he is Associate Professor and the Holder of the Dietz Career Development Professorship II. After the Ph.D. degree, he was with SatCon Technology Corporation, Cambridge, MA, for three years. His current research interests include the analysis, design, and real-time control of mechatronic systems, networked control systems, and nanoscale engineering and technology. He is the holder of three U.S. patents on precision positioning systems. Dr. Kim is a Member of Pi Tau Sigma and American Society of Mechanical Engineers (ASME) and a Senior Member of Institute of Electrical and Electronics Engineers (IEEE). He is a Primary Member of the ASME Mechatronics Technical Committee and a Member of the IEEE Nanotechnology Council. He was the Recipient of Korean Institute of Electrical Engineers' Student Paper Contest grand prize in 1988, Samsung Electronics' Humantech Thesis gold prize for his MIT dissertation in 1997, the NASA Space Act Award in 2002, and the 2005 Professional Engineering Publishing Award for the best paper published in 2004 in *Journal of Engineering Manufacture*. He was also a Semifinalist of the National Institute of Standards and Technology (NIST)'s Advanced Technology Program competition in 2000. He was appointed a Select Young Faculty Fellow by TAMU College of Engineering and the Texas Engineering Experiment Station twice in 2003 and 2005. He received the BP Teaching Excellence Award by TAMU College of Engineering in 2006.